



HAL
open science

REGIONAL OCEAN TIDE LOADING MODELING AROUND THE IBERIAN PENINSULA

M. Benavent, J. Arnos, F.G. Montesinos

► **To cite this version:**

M. Benavent, J. Arnos, F.G. Montesinos. REGIONAL OCEAN TIDE LOADING MODELING AROUND THE IBERIAN PENINSULA. *Journal of Geodynamics*, 2009, 48 (3-5), pp.132. 10.1016/j.jog.2009.09.023 . hal-00594436

HAL Id: hal-00594436

<https://hal.science/hal-00594436>

Submitted on 20 May 2011

HAL is a multi-disciplinary open access archive for the deposit and dissemination of scientific research documents, whether they are published or not. The documents may come from teaching and research institutions in France or abroad, or from public or private research centers.

L'archive ouverte pluridisciplinaire **HAL**, est destinée au dépôt et à la diffusion de documents scientifiques de niveau recherche, publiés ou non, émanant des établissements d'enseignement et de recherche français ou étrangers, des laboratoires publics ou privés.

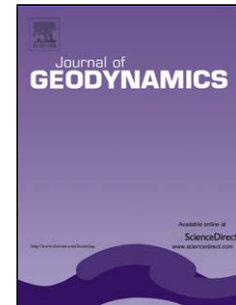
Accepted Manuscript

Title: REGIONAL OCEAN TIDE LOADING MODELING
AROUND THE IBERIAN PENINSULA

Authors: M. Benavent, J. Arnosó, F.G. Montesinos

PII: S0264-3707(09)00090-8
DOI: doi:10.1016/j.jog.2009.09.023
Reference: GEOD 917

To appear in: *Journal of Geodynamics*



Please cite this article as: Benavent, M., Arnosó, J., Montesinos, F.G., REGIONAL OCEAN TIDE LOADING MODELING AROUND THE IBERIAN PENINSULA, *Journal of Geodynamics* (2008), doi:10.1016/j.jog.2009.09.023

This is a PDF file of an unedited manuscript that has been accepted for publication. As a service to our customers we are providing this early version of the manuscript. The manuscript will undergo copyediting, typesetting, and review of the resulting proof before it is published in its final form. Please note that during the production process errors may be discovered which could affect the content, and all legal disclaimers that apply to the journal pertain.

REGIONAL OCEAN TIDE LOADING MODELING AROUND THE IBERIAN PENINSULA

M. Benavent^{*}, J. Arnosó, F. G. Montesinos

Instituto de Astronomía y Geodesia (CSIC-UCM). Facultad de Matemáticas. Plaza de Ciencias, 3. 28040 Madrid, Spain.

Abstract

We developed a new 1/12-degree resolution oceanic tide model in the complex region that surrounds the Iberian Peninsula. The model, named IBER01, allows us to obtain more accurate tidal loading computations for precise geodetic and gravimetric observations in this area. The modeling follows the scheme of data assimilation (coastal tide gauge, bottom pressure sensors and TOPEX/Poseidon altimetry) into a hydrodynamical model, which is based on two dimensional barotropic depth averaged shallow-water equations. Detailed bathymetry data and quadratic bottom friction with a specific drag coefficient for the region have been considered. Improved ocean load maps for the Iberian Peninsula are obtained for 8 harmonic constituents (Q1, P1, O1, K1, N2, M2, S2, K2), after computing the load effect (Newtonian attraction and elastic contribution) using IBER01 and six present-day global oceanic tide models for comparison. The results achieved verify the quality of the new model. Our ocean loading computations reduce considerably the discrepancies between the theoretical Earth tide parameters and those from observations at the level of 0.3%.

^{*} corresponding author
Fax: 34 913944615
e-mail: maite_benavent@mat.ucm.es

Keywords: Oceanic model; tidal loading; Iberian Peninsula; Earth tide

1. Introduction

The load effect of the ocean tides is one significant contribution to geophysical and geodetic measurements, particularly on Earth based gravimetric observations. Therefore, accurate computations of the tidal loading are required to correct high resolution gravity data before they can be used for further researches over timescales from hours to years (e.g. Neumeier et al., 2005). In turn, ocean tide models are the main error source in the tidal loading computations, especially where the ocean tide amplitudes are large (e.g. Sato et al., 2008; Arnosó et al., 2006; Neumeier et al., 2005; Baker and Bos, 2003).

The main goal of this work is to obtain more accurate ocean tide loading calculations for the Iberian Peninsula. Having into account the complex coastal geometry and surrounding bathymetry, which characterize the large ocean tides and their complex propagation pattern in the region, accurate load computations are obtained by developing a new regional ocean tide model, called IBER01¹. The model is based on altimetry measurements and tide gauge data assimilated into a hydrodynamical model, together with a further refinement of the ocean grid around calculation points, based on high resolution coastline data.

Previous studies in the area were carried out by Vieira et al. (1985a, 1985b) who made the first effort to model ocean tides in the region. They built up cotidal and corange maps for M2 and S2 waves by linking the harmonic constants derived from tide gauge measurements available in the region with the Schwiderski global model (Schwiderski, 1980). Francis and Melchior (1996), based on the relationship of the load effects using the Schwiderski model and the first global models derived from TOPEX/POSEIDON satellite altimetry data, they highlighted the need to improve ocean tide models in this particularly complex region. Although nowadays a large

¹ To request a copy of IBER01 model, please contact to the authors (maite_benavent@mat.ucm.es, jose_arnoso@mat.ucm.es, fuensanta_gonzalez@mat.ucm.es).

number of global models are available, there still exist discrepancies between them at different regions of the world (Baker and Bos, 2003), mainly due to their low spatial resolution and poor fit to the coastline (Arnosó et al., 2006; Neumeyer et al., 2005; Boy et al., 2003). We try to overcome these divergences with the model IBER01 presented here.

In the next section we deal with the key features of the oceanic model IBER01 and the modelling procedure. Section 3 is dedicated to ocean tide load computations, based on IBER01 and several recent global ocean tide models. Finally, the main findings of this study are summarized in Section 4.

2. The regional ocean tide model IBER01.

Model IBER01 covers the region of the Iberian Peninsula limited by 16°W-6°E in longitude and 34°N-48°N in latitude (see Figure 1). The model grid is 1/12° × 1/12°, which gives a resolution of about 9 kilometers. Figure 1 shows the bathymetry in the region obtained by averaging 1 minute Digital Atlas GEBCO (IOC, IHO and BODC, 2003) in the model grid. Model IBER01 is obtained by assimilating data from satellite altimetry and tide gauges into a hydrodynamical model, based on the non-linear 2D barotropic depth averaged shallow water equations. The governing equations for mass and momentum conservation, which include inertial terms, the quadratic bottom friction dissipation with drag coefficient set to $c_D = 0.003$ (e.g. Wang, 1993) and the horizontal viscosity terms with coefficient $A_H = 200 \text{ m}^2\text{s}^{-1}$ are given as (e.g. Andersen et al., 2006a)

$$\begin{aligned} \frac{\partial \zeta}{\partial t} &= -\nabla \cdot \mathbf{U} \\ \frac{\partial \mathbf{U}}{\partial t} + f\mathbf{k} \times \mathbf{U} + \mathbf{F} + \mathbf{U} \cdot \nabla \mathbf{u} + A_H \nabla^2 \mathbf{U} &= -gH \nabla (\zeta - \bar{\zeta}) \end{aligned} \quad (1)$$

where ζ is the ocean tide height, \mathbf{U} and \mathbf{u} are the tidal volume transport vector and the depth-averaged tidal velocity, respectively. Term f is the Coriolis parameter, \mathbf{k} is a unit vector in the vertical direction, \mathbf{F} is the quadratic bottom friction given by $\mathbf{F} = c_D (|\mathbf{u}|/H) \mathbf{U}$, H being the total water depth. The term $\bar{\zeta}$ expresses the equilibrium tide that includes one part derived from the astronomical tide-generating potential with allowance for the Earth's body tide, and a second part accounting for ocean tide loading computed from TPXO6.2 global model (Egbert and Erofeeva, 2002). The system of equations is solved by time-stepping using a finite difference scheme and setting the tidal elevations taken from the model GOT00.2 (Ray, 1999) at the open boundaries, that is, the limits of the model domain lying on sea water. To compute the a priori dynamical error covariance, which provides information about the magnitude and the spatial characteristic of the errors in the hydrodynamic model and the boundary conditions, a constant decorrelation length scale of 50 km is assumed (e.g., Egbert and Erofeeva, 2002).

Assimilated data consist of 87 coastal tide gauges and bottom pressure sensor measurements provided by several sources. We also use 12 years of TOPEX/Poseidon satellite altimetry data (364 cycles from 1992 to 2004) provided by the Pathfinder data base (Koblinsky et al., 1999) for 2400 selected data points. They include all along track data points taken with the original spacing of 7 km, which is comparable to the spatial resolution of the hydrodynamical model, and 36 crossover points in the model domain (see Figure 1). Amplitudes and phases of tidal constituents from tide gauge data and satellite altimeter measurements are estimated using tidal harmonic analysis of the time series at each point. The assimilation scheme is based on the *Representer Method* (Egbert and Erofeeva, 2002) that solves generalized inversion problems and is carried out with the OSU tidal inversion software (Egbert and Erofeeva, 2006). The assimilated tidal solution is obtained by minimizing a quadratic function, which is the sum of the squares of the misfits between the hydrodynamical model and data weighted with their corresponding a priori error covariances (e.g., Egbert and Bennet, 1996; Zaron and Egbert, 2007;

Zu et al., 2008). Data errors assumed in the assimilation scheme correspond to the mean square deviations estimated for each tidal wave through the least squares adjustment carried out in the tidal analysis process of the observed time series.

According to this procedure, model IBER01 is developed for eight harmonic constituents: Q1, O1, P1, K1, N2, M2, S2 and K2. The ocean tide regime in the region is dominated by the semidiurnal constituent M2 (see Figure 2), with amplitudes ranging from 1.7 m in the Atlantic French coast, 1 m around the Portuguese coast, decreasing sharply through the Gibraltar Strait and reaching only a few centimeters in the Mediterranean Sea. For this wave, phases propagate from south to north in the Atlantic area, while in the Mediterranean region they propagate towards NE with a fast phase variation. Other main semidiurnal constituents show similar spatial distribution in this region, although their tidal amplitudes are smaller than M2. Diurnal constituents differ substantially from the semidiurnal ones and exhibit a more complex pattern.

The Monte Carlo simulation approach (Dushaw et al., 1997) is used to estimate posterior errors for IBER01 model. The simulation consists of the inversion of synthetic data generated from the hydrodynamical equations (1) solving them using random forcing and boundary conditions with the a priori dynamical error covariance. After the inversion process, the difference between both synthetic solutions (dynamical and inverse) provides an estimation of the error in the ocean tide model (e.g., see Egbert and Erofeeva, 2002). Subsequent iterations of this process allow us to compute the posterior error variances. Figure 3 shows the respective standard deviations for M2 and O1 constituents. For all waves the large values are found in a few specific areas: the continental shelf of the Gulf of Biscay, the Galician coast and the Strait of Gibraltar (see locations in Figure 1). For instance, the standard deviation of IBER01 reaches up to 2% of the tidal amplitude in the Gulf of Biscay. It must be mentioned that these amplitudes are fast amplified over the wide continental shelf towards the coast, in such a way that significant

amplitude differences have been found at tide gauge locations when compared to satellite observations (see for instance Wöppelmann et al., 2006).

3. Ocean tide load calculations in the Iberian Peninsula

We calculate the gravity ocean tide loading and attraction effects in the Iberian Peninsula using the high resolution regional model IBER01 that supplements six global ocean tide models for comparison: FES2004 (Lyard et al., 2006), TPXO7.1 (Egbert and Erofeeva, 2002), CSR4.0 (Eanes and Bettadpur, 1995), AG2006 (Andersen et al., 2006b), GOT00.2 (Ray, 1999) and GOT4.7 (Ray, personal communication). The tidal load computations are carried out using a new software, which allows the combination of global and regional ocean models and a further refinement of the oceanic grid around calculation points situated near the coast, based on high resolution land/ocean mask data file. Such refinement could be done even at much larger distances from the coast if the calculation points were sensitive to the complex coastline and bathymetry. The computer program is written in FORTRAN and Visual Basic 6.0 as a visual interface for Windows users. The load effect L (Newtonian attraction and elastic contribution due to the Earth's surface displacement and mass redistribution) is computed based on the classical Farrell's procedure (Farrell, 1972), through the convolution of the ocean tide height, ζ , with the corresponding Green's functions G , as follows:

$$L(\vec{r}) = \rho_w \iint_{\Omega} \zeta(\vec{r}') G(|\vec{r} - \vec{r}'|) d\Omega \quad (2)$$

Where \vec{r} and \vec{r}' are the position vectors on the Earth's surface at the calculation and the loading point, respectively. ρ_w is the density of the sea water and $d\Omega$ the surface area element. In this study, we use the Green's functions given by Jentzsch (1997) for the PREM (Dziewonski and Anderson, 1981) Earth model with continental crust.

To get a more thorough modelling of the tidal load effect, the oceanic grid is refined around the calculation points within a selected radius, by using the high resolution land/water mask file derived from the 1 minute GEBCO Digital Atlas (IOC, IHO and BODC, 2003). The refinement radius is set depending on the distance to the coast from the calculation point. Within the selected radius, each oceanic grid cell is recursively subdivided into 4 smaller sub-cells until the distance from the sub-cell to the calculation point is greater than 20 times the radius of the sub-cell, following the recommendations given in Bos (2000).

3.1. Results

Figure 4 illustrates the amplitudes and phases of the gravity tide loading and attraction effects in the Iberian Peninsula, using the FES2004 ocean tide model supplemented with IBER01, for M2 and O1 waves. The ocean load amplitudes increase towards the Northwest and the phases propagate in NE-SW direction. Tidal loading are dominated by the semidiurnal constituent M2, with amplitudes ranging between 24 nms^{-2} and 90 nms^{-2} , whereas for the diurnal constituent O1 amplitudes reach a maximum value of some 5.2 nms^{-2} .

It must be emphasized that the contribution of the regional model IBER01 to the total ocean tide loading is about 83% at the north of the Peninsula and is reduced to 50% at its center. In this sense, the difference between load computations based only on global oceanic models and the ones using IBER01 supplementing the six global models becomes small. These differences are reduced to 0.1 nms^{-2} for N2 wave, 0.4 nms^{-2} for M2, 0.3 nms^{-2} for S2, 0.4 nms^{-2} for K2, 0.2 nms^{-2} for Q1, 0.2 nms^{-2} for O1, 0.1 nms^{-2} for P1 and 0.4 nms^{-2} for K1. In the case of M2 for instance, the maximum difference found in load computations using only global ocean models is about 13 nms^{-2} (16% of the load effect) near the Atlantic coast. The differences in phases, however, are found larger near the Mediterranean Sea. Assuming an accuracy of 1-2% in the loading computations (Bos and Baker, 2005), the differences in loading values obtained using only

global models without IBER01 are significantly higher than the errors in the loading computations.

As we mentioned before, the oceanic tide is one of the main contributions on gravity observations. In the Iberian Peninsula, the observed tidal gravity amplitudes for the principal semidiurnal wave M2 typically ranges between 450 to 550 nms^{-2} and 2° to 13° in phases, whereas for O1 the amplitude is in the range of 330 to 370 nms^{-2} (phases between -1° to 4° degrees). In our case, the gravity contribution from the sea reaches upon the 19% at the Atlantic coast, decreasing until 5% at the Mediterranean coast (see Figure 4). Even at the center of the Peninsula the gravity load amplitude can reach almost 10% of the gravity tide signal for the main harmonic constituent M2. To illustrate this effect we consider new gravity tide measurements made for a period of six months at two stations located in the area of Madrid: Valle-Absoluta (V-ABS) and Pilar-IAG (P-IAG) (see Figure 1). Both stations are the ends of a precise gravity calibration line, where absolute gravity measurements are performed periodically (Vieira et al., 1992; 1994; 2002). Results for V-ABS and P-IAG stations were obtained after processing recent data series of about six months in length with LaCoste&Romberg Graviton-EG1194 gravimeter (Arnosó et al., 2008), normalized in Valle de los Caídos tidal factors (Vieira et al., 1985c). Tidal analysis was performed with VAV program (Venedikov et al., 2003; 2005) using Tamura (1987) tide generating potential. Table 1 shows the results of the tidal analysis for main tidal waves O1 and M2 at both stations. For harmonic M2 the magnitude of the ocean loading is about 9% of the observed tidal amplitudes at both sites, whereas for harmonic O1 this magnitude is slightly below 1%. Figure 5 shows the computed load and the gravity tide residuals for a period of 8 days at these two locations. The residuals are obtained after subtracting the theoretical tide from the observed gravity, computed on the basis of the DDW model by Dehant et al., (1999) for a slightly elliptical, rotating inelastic/non hydrostatic Earth. The effect of the air pressure variation obtained at both stations was also subtracted. The magnitude of the oceanic loading effect and

the correlation between the two curves is clearly noted, although the residuals contain non-modeled effects such as local site perturbations and other atmospheric contributions. By using the program VAV we perform the tidal analysis of the gravity data. Results of load computation allow us to correct the observed tidal gravity factors and to determine the differences with the theoretical factor computed on the basis of the DDW inelastic Earth model. Thus, if we consider the mean value of the corrected gravimetric factors (from the six oceanic models supplemented with IBER01) the discrepancies with theoretical DDW model are -0.3% (V-ABS) and 0.02% (P-IAG) for the M2 wave. For O1 the discrepancies are -0.2% (V-ABS) and -0.3% (P-IAG).

4. Conclusions

A new high resolution ($1/12^\circ \times 1/12^\circ$) ocean tide model was developed for eight harmonic constituents (Q1, O1, P1, K1, N2, M2, S2 and K2) in the region of the Iberian Peninsula, which improves considerably previous regional ocean tide models. We used the most recent data assimilation techniques, on satellite altimetry and tide gauge observations together with detailed bathymetry data. For the dominant harmonic constituent M2, the standard deviation of IBER01 is in the range of 0.2 cm to 3.2 cm. The results obtained suggest further modelling of ocean tides for some isolated areas to deal with their specific characteristics.

Model IBER01, supplementing present-day global ocean tide models, allows us to compute accurate ocean load maps for eight harmonic constituents in the Iberian Peninsula. Therefore, the ocean load estimation for precise geodetic and gravimetric measurements can be improved considerably. We report here results from gravity tide observations made recently at stations placed at the centre of the Iberian Peninsula, where the magnitude of the oceanic loading effect is considerably large.

Acknowledgements

Projects PIE-200730I029 of the Spanish CSIC and CCG07-UCM/AMB-2783 of Spanish UCM-CAM have partially supported this work. We would like to express our thanks to the following organizations for providing tide gauge data series: IEO, PE and IHM from Spain, IHMP, IPCC from Portugal, BODC and HO from United Kingdom, IFREMER, SONEL and SHOM from France. We are greatly acknowledged to Spiros Pagiatakis, Nicolas Florsch and an anonymous referee for their thorough and constructive reviews, which improve considerably the manuscript.

References

- Andersen, O.B., Egbert, G., Erofeeva, L., Ray, R.D., 2006a. Mapping non linear shallow-water tides: a look at the past and future. *Oc. Dyn.*, 56, 416-429. DOI: 10.1007/s10236-006-0060-7.
- Andersen, O.B., Egbert, G., Erofeeva, L., Ray, R.D., 2006b. Non-linear tides in shallow water regions from multi-mission satellite altimetry & the Andersen 06 Global Ocean Tide Model. AGU WPGM meeting, Beijing, China, July, 2006.
- Arnosó, J., Benavent, M., Ducarme, B., Montesinos, F.G., 2006. A new ocean tide loading model in the Canary Islands region. *J. Geodyn.*, 41, 100-111.
- Arnosó, J., Montesinos, F.G., Benavent, M., Vélez, E.J., 2008. Gravity tide measurements at two absolute gravity sites in Madrid. *Proc. 6^a Asam. Hispano Portuguesa de Geodesia y Geofísica*, Tomar (Portugal), Febrero 2008, 257.
- Baker, T.F., Bos, M.S., 2003. Validating Earth and ocean tide models using tidal gravity measurements. *Geophys. J. Int.*, 152 (2), 468-485.
- Bos, M.S., 2000. Ocean tide loading using improved ocean tide models. PhD. Thesis, 203pp, University of Liverpool.
- Bos, M.S., Baker, T.F., 2005. An estimate of the errors in gravity ocean tide loading computations. *J. Geodyn.*, 79, 50-63.

- Boy, J.P., Llubes, M., Hinderer, J., Florsch, N., 2003. A comparison of tidal ocean loading models using superconducting gravimeter data. *J. Geophys. Res.*, 108 (B4), 2193, doi:10.1029/2002JB002050.
- Dehant, V., Defraigne, P., Wahr, J.M., 1999. Tides for a convective Earth. *J. Geophys. Res.*, 104, 1035-1058.
- Dushaw, B.D., Egbert, G.D., Worcester, P.F., Cornuelle, B.D., Howe, B.M., Metzger, K., 1997. A TOPEX/POSEIDON global tidal model (TPXO.2) and barotropic tidal currents determined from long-range acoustic transmissions. *Prog. Oceanog.*, 40, 337-367.
- Dziewonski, A.D., Anderson, D.L., 1981. Preliminary Reference Earth Model. *Phys. Earth Planet. Inter.* 25, 297-356.
- Eanes, R.J., Bettadpur, S., 1995. The CSR3.0 global ocean tide model. CSR-TM-95-06. Center for Space Research. Univ. of Texas, Austin.
- Egbert, G.D., Bennet, A.F., 1996. Data assimilation methods for ocean tides. In: P. Malanotte-Rizzoli (Ed.), *Modern Approaches to Data Assimilation in Ocean Modelling*, Elsevier Science, 147-179.
- Egbert, G.D., Erofeeva, S.Y., 2002. Efficient inverse modeling of barotropic ocean tides. *J. Ocean. Atmos. Tech.*, 19 (2), 183-204.
- Egbert, G.D., Erofeeva, S.Y., 2006. OSU Tidal Inversion software Documentation: OTIS version 3.2. Oregon State University, College of Oceanic and Atmospheric Sciences, Corvallis, Oregon.
- Farrell, W.E., 1972. Deformation of the Earth by Surface Loads. *Rev. Geophys. Space Phys.*, 10, 761-797.
- Francis, O., Melchior, P., 1996. Tidal loading in south Western Europe: A test area. *Geophys. Res. Lett.*, 23 (17), 2251-2254.

- IOC, IHO and BODC, 2003. Centenary Edition of the GEBCO Digital Atlas, published on CD-ROM on behalf of the Intergovernmental Oceanographic Commission and the International Hydrographic Organization as part of the General Bathymetric Chart of the Oceans, British Oceanographic Data Centre, Liverpool, U.K.
- Jentzsch, G., 1997. Earth tides and ocean tidal loading. In: Wilhelm, H., Zürn, W., Wenzel, H.G. (Eds.), *Tidal Phenomena, Lecture Notes in Earth Sciences*, Springer, Berlin Heidelberg New York, 66, 145-172.
- Koblinsky, C.J., Ray, R.D., Beckeley, B.D., Wang, Y.M., Tsaoussi, L., Brenner, A., Williamson, R., 1999. NASA ocean altimeter Pathfinder project report 1: Data processing handbook, NASA/TM-1998-208605.
- Lyard, F., Lefevre, F., Letellier, T., Francis, O., 2006. Modelling the global ocean tides: insights from FES2004. *Oc. Dyn.*, 56 (5-6), 394-415.
- Neumeyer, J., del Pino, J., Sun, H.P., Hartmut, P., 2005. Improvement of ocean loading correction on gravity data with additional tide gauge measurements. *J. Geodyn.*, 40, 104-111.
- Ray, R.D., 1999. A global ocean tide model from TOPEX/Poseidon altimeter: GOT99.2. NASA Technical Memorandum, TM-209478, 58 pp.
- Sato, T., Miura, S., Ohta, Y., Fujimoto, H., Sun, W., Larsen, C.F., Heavner, M., Kaufman, A.M., Freymueller, J.T., 2008. Earth tides observed by gravity and GPS in southeastern Alaska. *J. Geodyn.*, 46, 78-89.
- Schwiderski, E.W., 1980. On charting global ocean tides. *Rev. Geophys. Space Phys.*, 18, 243-268.
- Tamura, Y., 1987. A harmonic development of the tide-generating potential. *Bull. Inf. Marées Terr.*, 99, 6813-6855.
- Venedikov, A.P., Arnosó, J., Vieira, R., 2003. VAV: a program for tidal data processing. *Comput. Geosci.* 29, 487-502.

- Venedikov, A.P., Arnosó J., Vieira, R., 2005. New version of program VAV for tidal data processing. *Comput. Geosci.*, 31, 667–669.
- Vieira, R., Toro, C., Megias, E., 1985a. Ocean maps in the nearby of the Iberian Peninsula. Part I: M2 Iberia Map. *Proc. Tenth Int. Symp. Earth Tides*. Consejo Sup. Investigaciones Científicas, Madrid, 679–695.
- Vieira, R., Toro, C., Fernandez, J., 1985b. Ocean maps in the nearby of the Iberian Peninsula. Part II: S2 Iberia Map. *Proc. Tenth Int. Symp. Earth Tides*. Consejo Sup. Investigaciones Científicas, Madrid, 697–706.
- Vieira, R., Torroja, J.M., Toro, C., 1985c. A general discussion about normalization of gravimeters in the Iberian gravity tide profile. *Proc. Tenth Int. Symp. Earth Tides*. Consejo Sup. Investigaciones Científicas, Madrid, 165–175.
- Vieira, R., Camacho, A.G., Toro, C., Montesinos, F.G., 1992. A calibration gravimetric lines between Madrid and Valle de los Caídos stations. *Comptes Rendus J.L.G. Conseil Europe*, 73, 18-25.
- Vieira, R., Camacho, A.G., Toro, C., Montesinos, F.G., Arnosó, J., Makinen, J., 1994. Línea de calibración Madrid-Valle. *Observaciones de gravedad absolutas. Conf. Inter. Geodesia y Cartografía. Maracaibo (Venezuela)*, I, 275-286, ISBN: 84-87.488-05-6.
- Vieira, R., Camacho A.G., Ortíz, E., 2002. Global adjustment for the Gravity Calibration Line Madrid-Valle de los Caidos. *Física de la Tierra*, 14, 127-159, ISSN: 0214-4557.
- Wang, D.P., 1993. The Strait of Gibraltar Model: internal tide, diurnal inequality and fortnightly modulation. *Deep-Sea Res. I*, 40, 1187-1203.
- Wöppelmann, G., Zerbini, S., Marcos, M., 2006. Tide gauges and geodesy: a secular synergy illustrated by three present-day case studies. *C. R. Geoscience*, 338, 980-991.
- Zaron, E.D., Egbert, G.D., 2007. The impact of the M2 internal tide on data-assimilative model estimates of the surface tide. *Ocean Modelling*, 18, 210-216.

Zu, T., Gan, J., Erofeeva, S.Y., 2008. Numerical study of the tide and tidal dynamics in the South China Sea. *Deep-Sea Res. I-Oceanographic Research Papers*, 55 (2), 137-154.

Accepted Manuscript

Figure captions

Figure 1. Limits of the model domain and bathymetry used for the regional ocean tide model IBER01. Black circles show the location of the tide gauges and white traces represent TOPEX/POSEIDON ground tracks assimilated in the model. The crosses show the location of the tidal gravity stations V-ABS and P-IAG in Madrid.

Figure 2. Cotidal chart (*left*) and corange maps (*right*) of M2 (*top*) and O1 (*bottom*) waves. Amplitudes are given in centimeters and phases, in degrees, are given with respect to Greenwich.

Figure 3. Standard deviations for M2 (*top*) and O1 (*bottom*) waves for the oceanic model IBER01.

Figure 4. Amplitudes (*left*) and local phases (*right*) of the computed tidal gravity loading based on the FES2004 global ocean model supplemented with regional model IBER01, for M2 and O1 tidal waves.

Figure 5. Observed tidal gravity residuals (*black curve*), after subtracting the theoretical tide computed on the basis of DDW inelastic Earth model, and ocean tide loading (*gray curve*), based on the oceanic models IBER01 and FES2004, at the observing sites P-IAG (*top*) and V-ABS (*bottom*).

Table captions

Table 1. Observed amplitudes (A), gravimetric factors (δ) and phase differences (α) for the O1 and M2 tidal waves, at the sites P-IAG and V-ABS. The tidal potential used is Tamura (1987). Amplitudes (L) and phases (λ) of the ocean tide loading, based on the six global oceanic models supplemented with IBER01. δ^C and α^C are the observed amplitude factors and phases after ocean loading correction. The mean corrected tidal gravity factors and the standard deviation are also listed. The DDW inelastic Earth model is given for comparison with δ^C values. Amplitudes are given in nms^{-2} and phases in degrees (local).

Accepted Manuscript

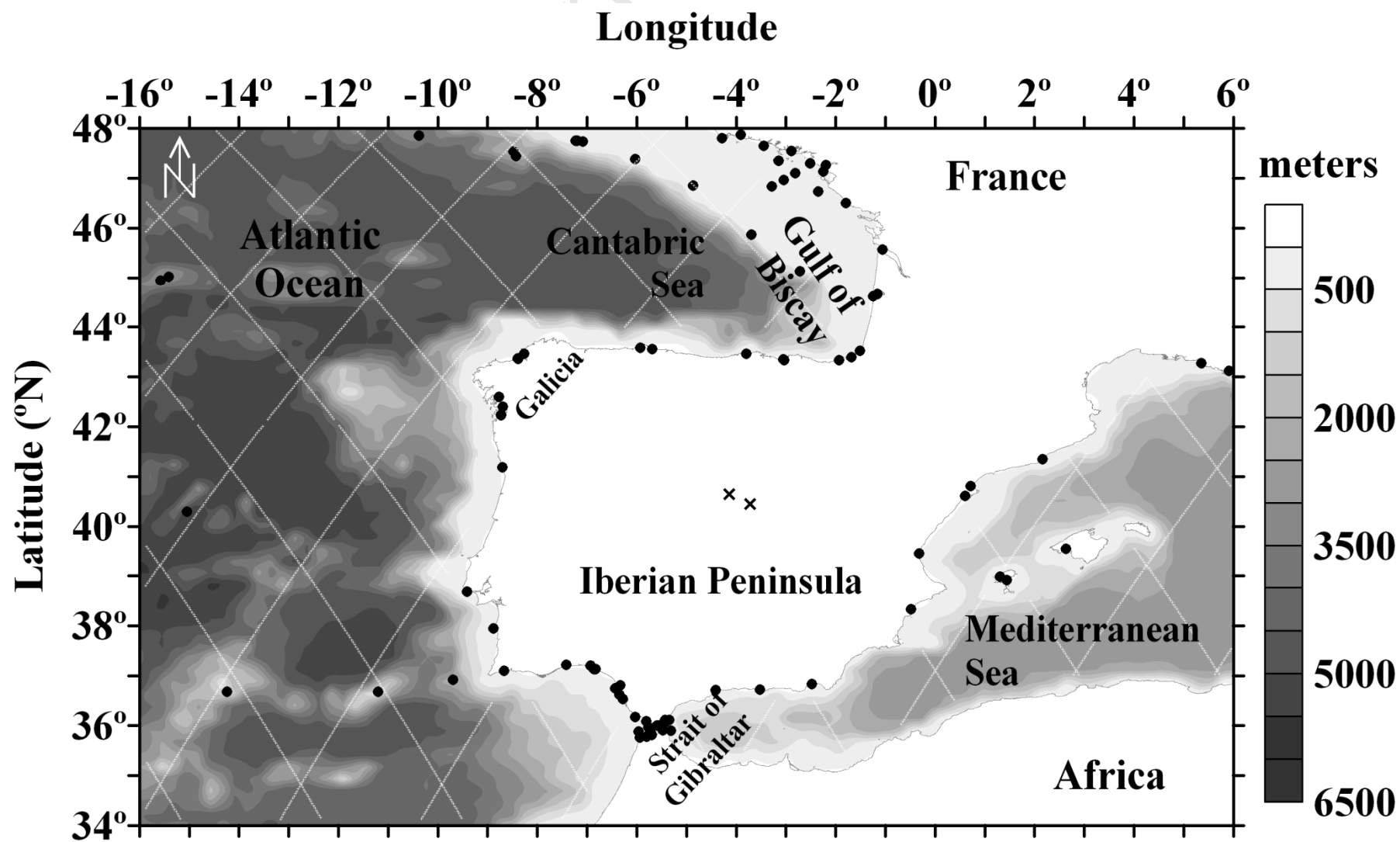


Figure 1

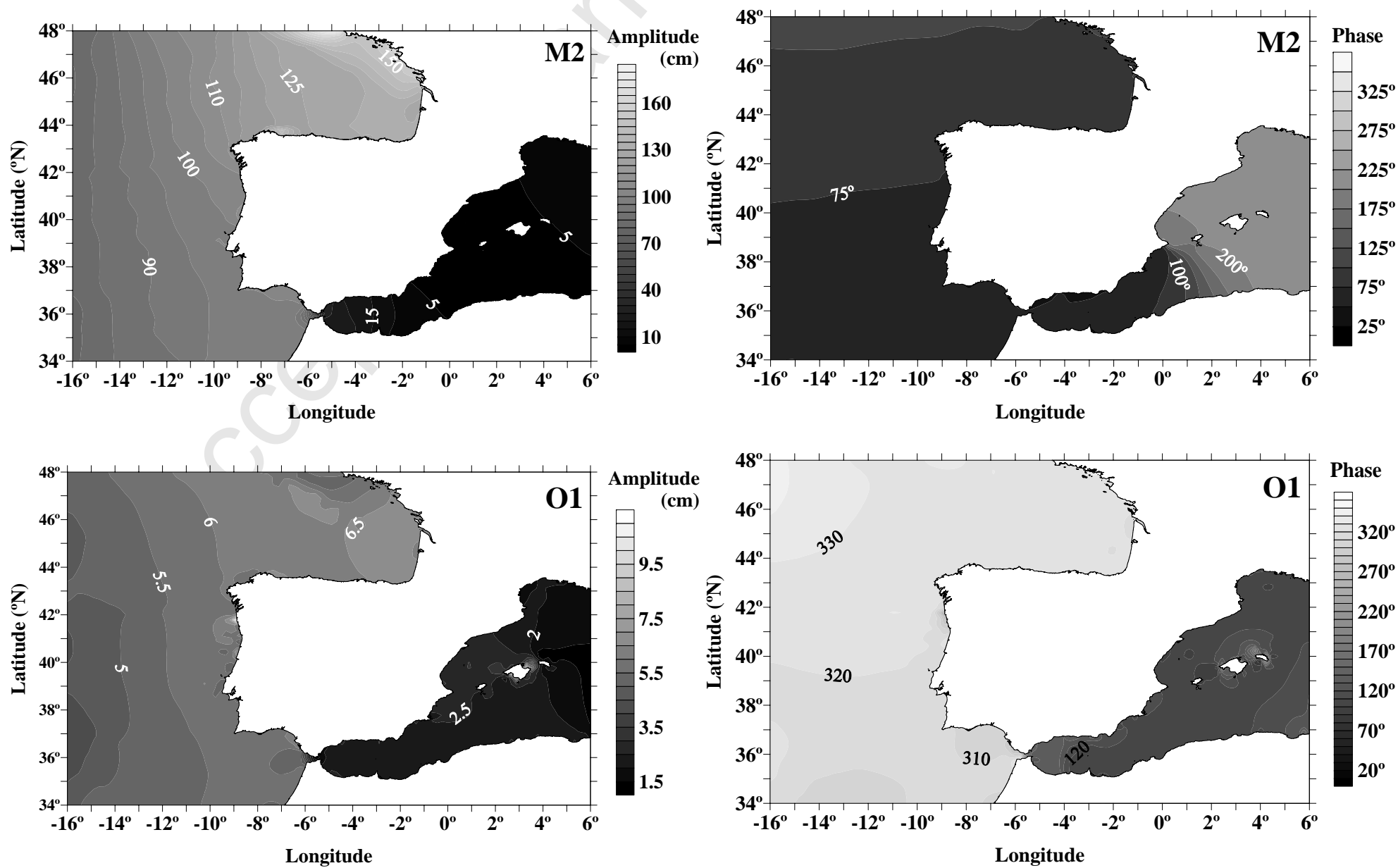


Figure 2

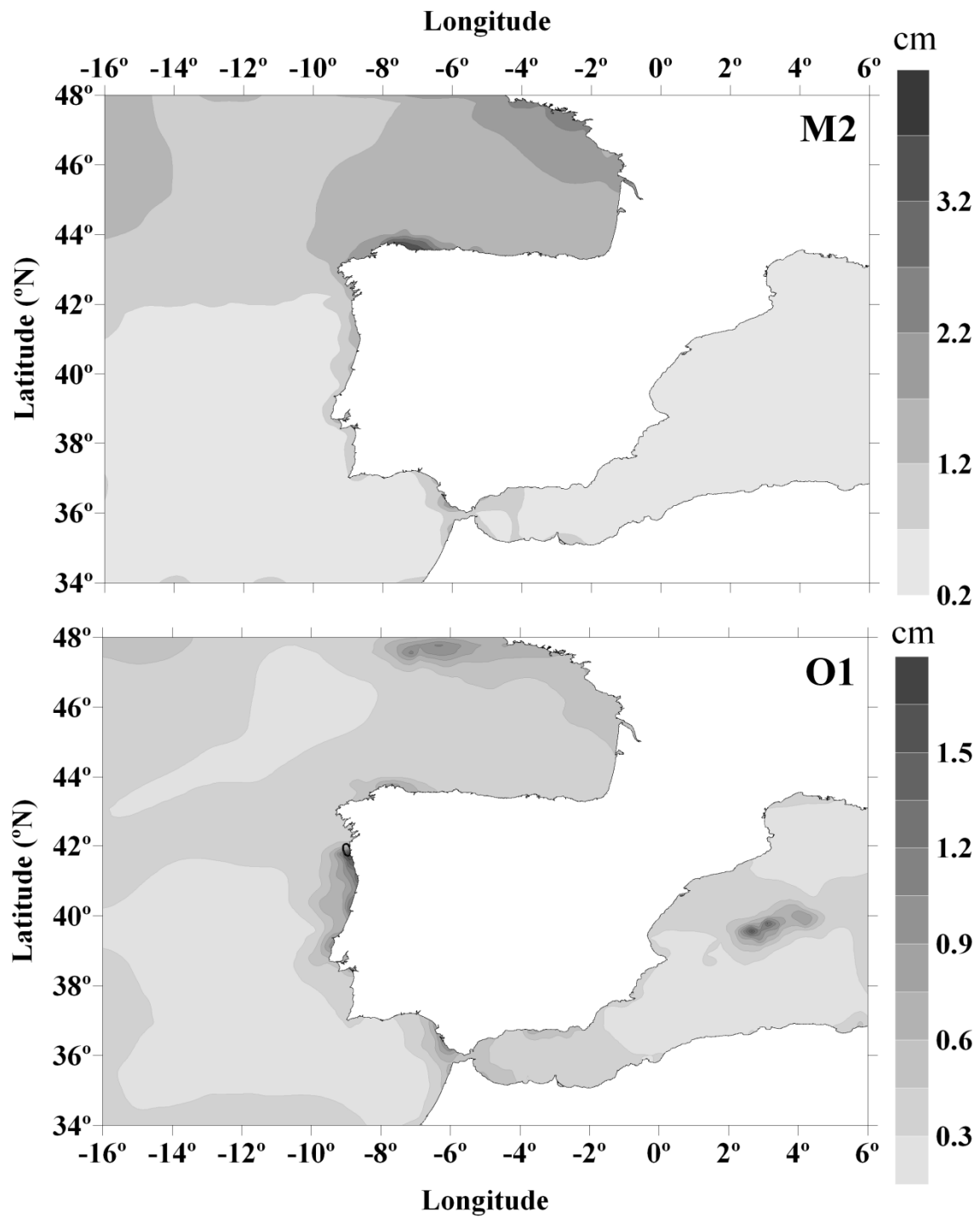


Figure 3

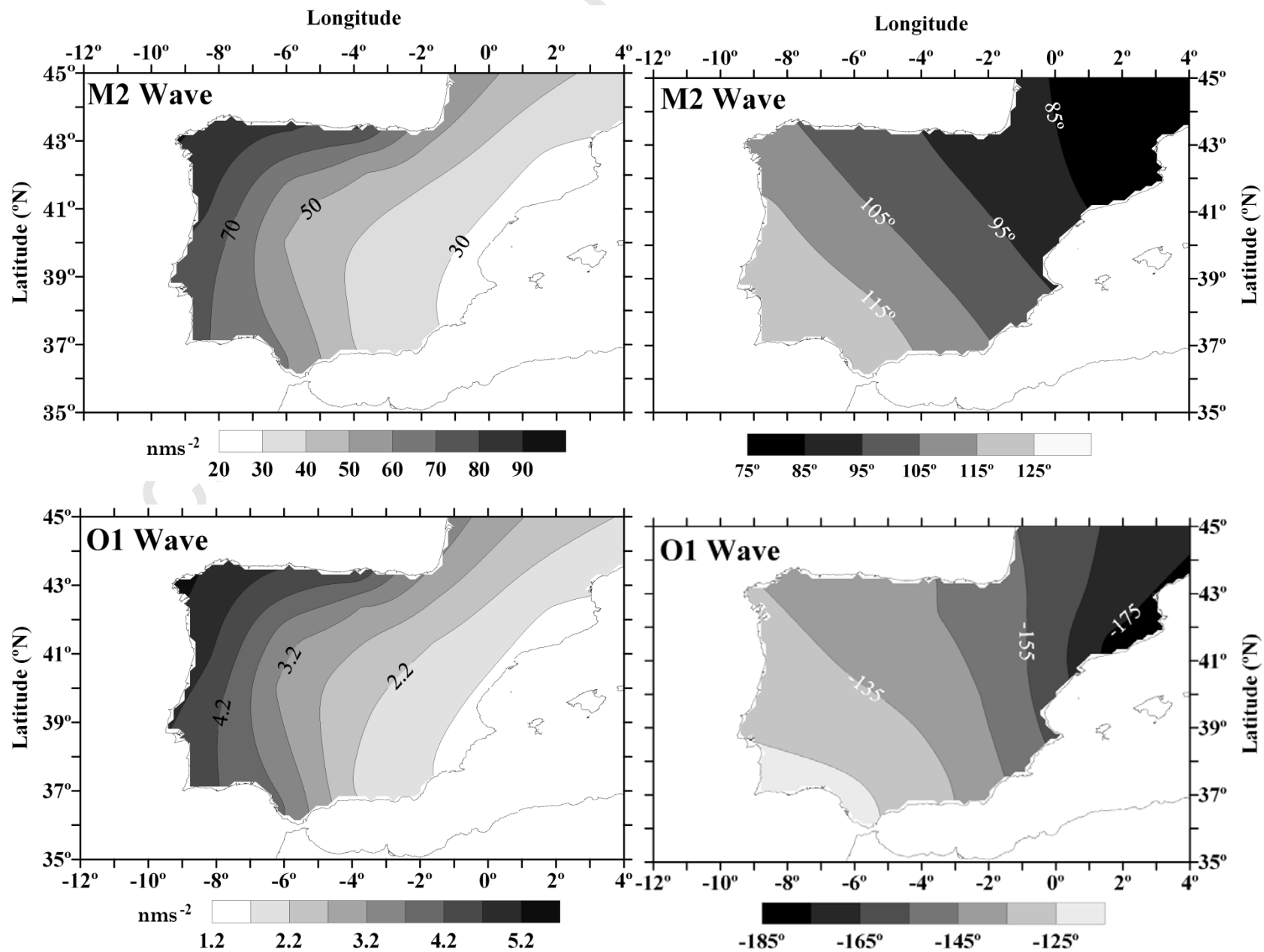


Figure 4

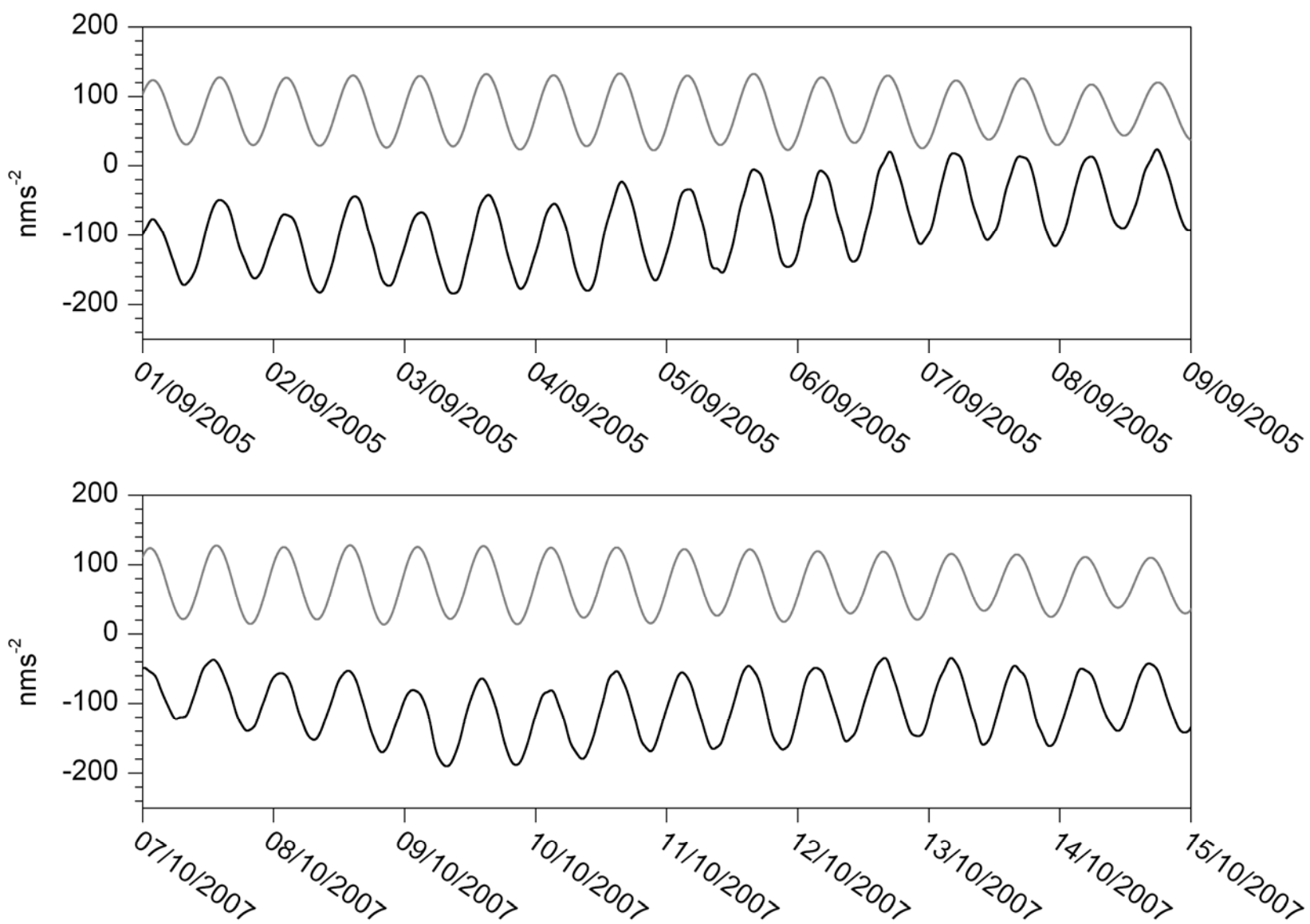


Figure 5

Observed	V-ABS								P-IAG							
	M2				O1				M2				O1			
	A	δ	α		A	δ	α		A	δ	α		A	δ	α	
	496.47	1.1482	4.775		353.11	1.1496	-0.403		498.75	1.1467	4.564		353.19	1.1518	-0.342	
	± 0.30	± 0.0007	± 0.035		± 0.42	± 0.0014	± 0.070		± 0.27	± 0.0006	± 0.031		± 0.30	± 0.0010	± 0.050	
Model+IBER01	δ^c	α^c	L	λ												
GOT00.2	1.16538	-0.110	43.28	102.20	1.15578	-0.141	2.50	-140.02	1.16165	-0.025	40.72	101.47	1.15767	-0.100	2.34	-140.64
CSR4.0	1.16598	-0.122	43.43	102.50	1.15591	-0.128	2.58	-139.23	1.16224	-0.037	40.88	101.79	1.15780	-0.088	2.42	-139.80
TPX07.1	1.16506	-0.127	43.39	101.98	1.15590	-0.166	2.43	-143.35	1.16132	-0.041	40.84	101.23	1.15779	-0.125	2.27	-144.22
FES2004	1.16552	-0.098	43.19	102.30	1.15660	-0.157	2.64	-145.19	1.16179	-0.013	40.63	101.58	1.15849	-0.116	2.48	-146.09
GOT4.7	1.16483	-0.134	43.43	101.83	1.15606	-0.187	2.40	-146.46	1.16110	-0.048	40.87	101.08	1.15795	-0.146	2.24	-147.53
AG2006	1.16584	-0.112	43.33	102.45	1.15582	-0.127	2.57	-138.70	1.16210	-0.028	40.79	101.73	1.15772	-0.085	2.41	-139.16
<i>MEAN</i>	1.16544	-0.117			1.15601	-0.151			1.16170	-0.032			1.1579	-0.110		
<i>STD</i>	0.00044	0.013			0.00030	0.024			0.00044	0.013			0.00030	0.024		
<i>DDW</i>	1.16189				1.15424				1.16189				1.15424			

Table 1